

CMS Draft Analysis Note

The content of this note is intended for CMS internal use and distribution only

2022/01/13

Archive Hash: d249620-D

Archive Date: 2022/01/13

Search for Higgs boson decays to long-lived scalar particles to SM τ final state with Regions of Interest construction

S. Kim³, T. Kolberg³, A. Hart², K. Rahman², Y. Gerstein², K. Peña¹, and L. Benato¹

¹ Deutsches Elektronen-Synchrotron

² Rutgers, The State University of New Jersey

³ Florida State University

Abstract

We present a search for long-lived particles (LLPs) produced in gluon fusion Higgs production mode (ggH), using the novel Regions of Interest strategy. Regions of Interest (ROIs) are formed as a collection of pair-wise track vertices fitted by the V0Fitter in CMSSW. The analysis focuses on lifetime of LLPs in the tracker region, with concentration on the ggH mode for the highest Higgs production cross-section. Variables of the constructed ROIs become inputs for our Deep Neural Network (DNN) Machine Learning (ML) algorithms, as a main discriminator between the signal and the background. We focus on the τ SM fermion final state. This final state is particularly interesting, given τ final state exclusion limits are frequently omitted in precedent analysis, due to τ fermions' non trivial final state reconstruction. No excess of events over the standard model expectation is observed. The results are interpreted in the context of exotic Higgs decays to a pair of long-lived scalars (S). We set limits on the branching ratio of the Higgs to LLPs, $\mathcal{B}(H \rightarrow SS)$, as a function of the proper lifetime.

This box is only visible in draft mode. Please make sure the values below make sense.

PDFAuthor:	S. Kim
PDFTitle:	Search for Higgs boson decays to long-lived scalar particles to SM τ final state with Regions of Interest construction
PDFSubject:	CMS
PDFKeywords:	CMS, physics

Please also verify that the abstract does not use any user defined symbols

Contents

1			
2	1	Introduction	2
3	2	Data and simulated samples	4
4	2.1	Data samples	4
5	2.2	Monte Carlo Samples	4
6	2.2.1	Signal Model and Simulation	4
7	2.2.2	Background Monte Carlo	5
8	3	Physics object definitions	8
9	3.1	Muons	8
10	3.2	Jets	8
11	3.3	Taus	8
12	3.4	Region of Interest	8
13	3.4.1	Tracks	9
14	3.4.2	Vertex Fitter	9
15	3.4.3	ROI formation	9
16	4	Event Selection, Signal and Control Regions	10
17	4.1	Global Tags	10
18	4.2	Trigger Strategy	10

1 Introduction

Discovery of particles at the electroweak scale, such as the top quark at Fermilab's CDF and D0 [1, 2] and the Higgs Boson at Large Hadron Collider (LHC) in CERN [3, 4], led to discovery of all constituents in the standard model (SM). SM helps to describe the nature of fundamental particles and their interactions with precision. In spite of its success, the SM suffers from a few obstacles. The evidence of neutrino mass and mixing [5], the observation of bullet clusters confirming the presence of dark matter (DM) [6–10], and baryon-antibaryon asymmetry [11] remain unsolved in framework of the SM. In addition, SM suffers from the naturalness problem. To solve all such issues, one needs to look for Beyond the Standard Model (BSM).

The naturalness problem originates from the fact that the Higgs of the SM is a scalar particle. Unlike fermions or gauge bosons, its mass is not protected by any symmetry and subject to large radiative corrections, especially from the top quark loop. Thus, for the SM to be valid up to the Planck or Grand Unification Theory (GUT) scale, the radiative corrections are enormous. One needs un-natural amount of fine tuning to fit the Higgs mass at the observed value of 125 GeV. One of the most popular solutions to this problem is Supersymmetry (SUSY), which assigns chirality to the Higgs particle. SUSY solves correction problem, neutrino masses, and provides candidate of DM. Unfortunately, LHC has found no significant excess over the SM background in their search for SUSY[?]. Although the non-observation of superpartners does not invalidate SUSY, it makes less attractive among the particle physics community. Non-observation of superpartners, particularly the stop (scalar partner of the top quark) has pushed its mass beyond 1 TeV. This generated problem of "little hierarchy", but an alternative solution of "neutral naturalness" remains.

In the framework of neutral naturalness, top partners are not charged under the SM color group. Because of being colorless, its cross-section of production is much less, and the present limits on the top partner particles are well below 1 TeV. Examples of neutral naturalness models are Twin Higgs [12], Folded SUSY [13], and Quirky Little Higgs [14]. Theoretical models provide the possibility of neutral Long Lived Particles (LLPs), which may be produced in the proton-proton collisions of the LHC and decay back to SM particles far from the interaction point (IP).[15] In the Mirror and Twin SM models, only SM Higgs boson can interact with both SM QCD and mirror QCD partners. If the mirror QCD gluons could form scalar glueballs, the SM Higgs boson can become "Higgs Portal" between the SM and BSM mirror QCD scalar glueballs. BSM mirror QCD scalar glueballs can only decay back to SM particles via Higgs portal as well. Because of its decay as an offshell Higgs boson, its crosssection is highly suppressed. Decay branching ratio to highest mass fermions will be highest following the Yukawa couplings. Decay ratio into b quarks or tau leptons are highest depending on the mirror scalar's mass. The displaced decays of the scalars will lead to exotic signatures in the LHC, such as distant innermost tracker hit, displaced vertices, and displaced jets. Phenomenology of long-lived particles in LHC entailed increase in interest of neutral naturalness framework among the particle physics community. [16, 17]. The long-lived scalar model is shown in the left-panel of Figure ??.

Searches for LLPs decaying into final states containing jets were investigated at the Tevatron ($\sqrt{s} = 1.96$ TeV) by both CDF [18] and D0 [19] Collaborations, at the LHC by the ATLAS and LHCb Collaborations at $\sqrt{s} = 7$ TeV [20, 21], by the ATLAS, CMS and LHCb Collaborations at $\sqrt{s} = 8$ TeV [22–28]. More recently, CMS Collaboration [29–34] and ATLAS Collaboration [35–46] at $\sqrt{s} = 13$ TeV. CMS Collaboration released a new result in 2021, in which Higgs are created in association with Z vector boson [47], for better probe into lighter scalar mass thanks to its clean dilepton trigger.

Although exclusion limit on b and d-quarks were set below 1 for analyses above, exclusion

limit for τ final state has been frequently omitted or presented with values above 1. Displaced Jets analyses face challenges for τ final state, due to τ 's non-trivial hadronic and leptonic decay mode and complicated reconstruction mechanism. However, Leptophilic model for Twin Higgs and other Higgs models are also highly motivated [48]. Continuous neglect of τ final state limit is not only a good practice, but overlooking an important undiscovered phase space. This analysis searches for Higgs Portal model with the Higgs' Leptophilic nature, which focuses on τ final state. The 55GeV maximum mass is to investigate only on-shell neutral scalar particles from the Higgs. Minimum 7GeV of scalar particles' mass is required to create on-shell tau-lepton pairs. Feynman diagram of the scalar particle production mechanism is depicted in figure 1.

Most CMS searches are not optimal for detecting Higgs boson decays to displaced-jets due to the soft p_T nature of its decays products – the new scalars. Low HT signature becomes particularly more difficult with long lived signature. Higgs produced in association with Z vector boson analysis [47] overcame this barrier with help of dilepton trigger. Although ggH production mode gives the largest Higgs crosssection, it complicates the trigger strategy even further. This analysis exploits the τ lepton's leptonic decay mode, in which the τ lepton decays into a soft muon, with trigger of B Parking HLT Path implemented in CMS for the year 2018 of Run2.

Another challenge for τ lepton analysis is different decay modes of τ leptons. τ leptons decay hadronically and leptonically with several different sub-decay modes. Developing analysis strategies to optimize search for each sub-decay modes are extremely complicated, a main reason for omission or no good exclusion limit in precedent LHC results. To be inclusive of all τ leptons' decay modes, displaced vertex search can be more efficient than displaced object (jet,muon,electrons). We exploit the newly developed Regions of Interest mechanism in the tracker volume. Regions of Interest (ROI) form displaced vertex candidates, by fitting pair-wise tracks of Lost-tracks and PackedPFCandidates classes in MINIAOD into a vertex. ROIs save all relevant track and fitted vertex qualities along with isolation information. These variables are used as input for Machine Learning (ML) algorithms, enabling a highly generic and data-scientific search method.

The rest of this note is organized as follows. In Section 2, we describe the datasets and Monte Carlo samples, including those of the signal model, used in the search. The physics objects and formation of Regions of Interest are described in Section 3. The trigger strategy and event selections are presented in Section 4. Section ?? describes the data driven background estimate and its validation. Section ?? describes the systematic uncertainties. Finally, Section ?? presents the results of the search. We conclude with Section ??.

2 Data and simulated samples

2.1 Data samples

The analysis uses B Parking datasets. Data was collected during 2018 of Run 2 and corresponds to an integrated luminosity of 41 fb^{-1} .

Table 1: Datasets used in the analysis: and 2018.

Data sample	Integrated Luminosity (fb^{-1})
/ParkingBPH1/Run2018A-05May2019-v1/MINIAOD	0.866
/ParkingBPH2/Run2018A-05May2019-v1/MINIAOD	0.866
/ParkingBPH3/Run2018A-05May2019-v1/MINIAOD	0.866
/ParkingBPH4/Run2018A-05May2019-v1/MINIAOD	0.866
/ParkingBPH5/Run2018A-05May2019-v1/MINIAOD	0.866
/ParkingBPH6/Run2018A-05May2019-v1/MINIAOD	0.866
Total	5.20
/ParkingBPH1/Run2018B-05May2019-v2/MINIAOD	1.083
/ParkingBPH2/Run2018B-05May2019-v2/MINIAOD	1.083
/ParkingBPH3/Run2018B-05May2019-v2/MINIAOD	1.083
/ParkingBPH4/Run2018B-05May2019-v2/MINIAOD	1.083
/ParkingBPH5/Run2018B-05May2019-v2/MINIAOD	1.083
/ParkingBPH6/Run2018B-05May2019-v2/MINIAOD	1.083
Total	6.49
/ParkingBPH1/Run2018C-05May2019-v1/MINIAOD	1.079
/ParkingBPH2/Run2018C-05May2019-v1/MINIAOD	1.079
/ParkingBPH3/Run2018C-05May2019-v1/MINIAOD	1.079
/ParkingBPH4/Run2018C-05May2019-v1/MINIAOD	1.079
/ParkingBPH5/Run2018C-05May2019-v1/MINIAOD	1.079
Total	5.39
/ParkingBPH1/Run2018D-05May2019promptD-v1/MINIAOD	6.542
/ParkingBPH2/Run2018D-05May2019promptD-v1/MINIAOD	6.542
/ParkingBPH3/Run2018D-05May2019promptD-v1/MINIAOD	6.542
/ParkingBPH4/Run2018D-05May2019promptD-v1/MINIAOD	6.542
/ParkingBPH5/Run2018D-05May2019promptD-v1/MINIAOD	6.542
Total	32.7
ParkingBPH Total	50.78

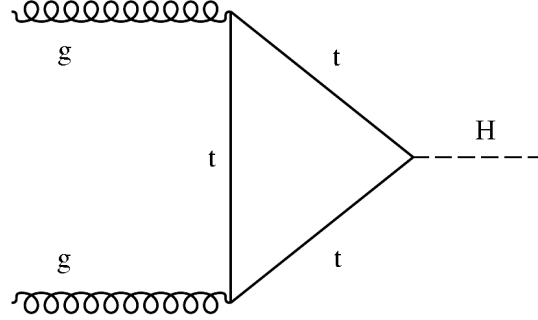
2.2 Monte Carlo Samples

2.2.1 Signal Model and Simulation

The ggH process (see Figure 1) is generated at next-to-next-to-leading order (NNLO) and next-to-next-to-leading-log (NNLL) QCD and next-to-leading order (NLO) EW accuracies [49]. The Higgs boson mass is set to 125 GeV for all signal samples. The cross sections, computed at NNLO+NNLL QCD and NLO EW accuracies and obtained from the CERN Report 3, are 4.414 pb. The CMS detector response is modeled with GEANT4 [50].

Table 2 lists the signal Monte Carlo samples.

Figure 1: Leading Feynman diagrams for ggH production mode

Table 2: $gg(h \rightarrow ss \rightarrow \tau\bar{\tau}\tau\bar{\tau})$ Signal Monte Carlo samples.

Sample
/ggH.HToSSTo4Tau.MH-125.TuneCP5.13TeV-powheg-pythia8/CAMPAIGN/MINIAODSIM
/ggH.HToSSTo4Tau.MH-125.MS-55.ctauS-1.TuneCP5.13TeV-powheg-pythia8/CAMPAIGN/MINIAODSIM
/ggH.HToSSTo4Tau.MH-125.MS-55.ctauS-10.TuneCP5.13TeV-powheg-pythia8/CAMPAIGN/MINIAODSIM
/ggH.HToSSTo4Tau.MH-125.MS-55.ctauS-100.TuneCP5.13TeV-powheg-pythia8/CAMPAIGN/MINIAODSIM
/ggH.HToSSTo4Tau.MH-125.MS-55.ctauS-1000.TuneCP5.13TeV-powheg-pythia8/CAMPAIGN/MINIAODSIM
/ggH.HToSSTo4Tau.MH-125.MS-40.ctauS-1.TuneCP5.13TeV-powheg-pythia8/CAMPAIGN/MINIAODSIM
/ggH.HToSSTo4Tau.MH-125.MS-40.ctauS-10.TuneCP5.13TeV-powheg-pythia8/CAMPAIGN/MINIAODSIM
/ggH.HToSSTo4Tau.MH-125.MS-40.ctauS-100.TuneCP5.13TeV-powheg-pythia8/CAMPAIGN/MINIAODSIM
/ggH.HToSSTo4Tau.MH-125.MS-40.ctauS-1000.TuneCP5.13TeV-powheg-pythia8/CAMPAIGN/MINIAODSIM
/ggH.HToSSTo4Tau.MH-125.MS-15.ctauS-1.TuneCP5.13TeV-powheg-pythia8/CAMPAIGN/MINIAODSIM
/ggH.HToSSTo4Tau.MH-125.MS-15.ctauS-10.TuneCP5.13TeV-powheg-pythia8/CAMPAIGN/MINIAODSIM
/ggH.HToSSTo4Tau.MH-125.MS-15.ctauS-100.TuneCP5.13TeV-powheg-pythia8/CAMPAIGN/MINIAODSIM
/ggH.HToSSTo4Tau.MH-125.MS-15.ctauS-1000.TuneCP5.13TeV-powheg-pythia8/CAMPAIGN/MINIAODSIM
/ggH.HToSSTo4Tau.MH-125.MS-7.ctauS-1.TuneCP5.13TeV-powheg-pythia8/CAMPAIGN/MINIAODSIM
/ggH.HToSSTo4Tau.MH-125.MS-7.ctauS-10.TuneCP5.13TeV-powheg-pythia8/CAMPAIGN/MINIAODSIM
/ggH.HToSSTo4Tau.MH-125.MS-7.ctauS-100.TuneCP5.13TeV-powheg-pythia8/CAMPAIGN/MINIAODSIM
/ggH.HToSSTo4Tau.MH-125.MS-7.ctauS-1000.TuneCP5.13TeV-powheg-pythia8/CAMPAIGN/MINIAODSIM

An example PYTHIA v8.230 fragment for the Higgs decay to scalars (scalars) and their subsequent decay to tau leptons is given below. In this example the mass of the scalar is 15 GeV and its lifetime ($c\tau$) is 10,000 mm.

```
'90000006:all = sk skbar 0 0 0 15 1.9732e-17 1.0 75.0 10000',
'90000006:oneChannel = 1 1.0 101 15 -15',
'90000006:mayDecay = on',
'90000006:isResonance = on',
'25:m0 = 125.0',
'25:onMode = off',
'25:addChannel = 1 0.000000001 101 90000006 -90000006',
'25:onIfMatch = 90000006 -90000006',
'90000006:onMode = off',
'90000006:onIfAny = 5',
```

2.2.2 Background Monte Carlo

All samples were processed as recommended in the PPD Run2 Analysis Guideline [51]. Tables ??-6 summarizes the background Monte Carlo used in this analysis.

a

Table 3: QCD MuEnriched Pt5 background Monte Carlo samples, RunIIAutumn18MiniAOD-102X_upgrade2018_realistic_v15

Sample
/QCD_Pt-15to20_MuEnrichedPt5_TuneCP5_13TeV_pythia8/*-v3/MINIAODSIM
/QCD_Pt-20to30_MuEnrichedPt5_TuneCP5_13TeV_pythia8/*-v4/MINIAODSIM
/QCD_Pt-30to50_MuEnrichedPt5_TuneCP5_13TeV_pythia8/*-v3/MINIAODSIM
/QCD_Pt-50to80_MuEnrichedPt5_TuneCP5_13TeV_pythia8/*-v3/MINIAODSIM
/QCD_Pt-80to120_MuEnrichedPt5_TuneCP5_13TeV_pythia8/*_ext1-v2/MINIAODSIM
/QCD_Pt-120to170_MuEnrichedPt5_TuneCP5_13TeV_pythia8/*_ext1-v2/MINIAODSIM
/QCD_Pt-170to300_MuEnrichedPt5_TuneCP5_13TeV_pythia8/*-v3/MINIAODSIM
/QCD_Pt-300to470_MuEnrichedPt5_TuneCP5_13TeV_pythia8/*_ext3-v1/MINIAODSIM
/QCD_Pt-470to600_MuEnrichedPt5_TuneCP5_13TeV_pythia8/*_ext1-v2/MINIAODSIM
/QCD_Pt-600to800_MuEnrichedPt5_TuneCP5_13TeV_pythia8/*-v1/MINIAODSIM
/QCD_Pt-800to1000_MuEnrichedPt5_TuneCP5_13TeV_pythia8/*_ext3-v2/MINIAODSIM
/QCD_Pt-1000toInf_MuEnrichedPt5_TuneCP5_13TeV_pythia8/*-v1/MINIAODSIM

Table 4: W,Z,H background Monte Carlo samples, RunIIAutumn18MiniAOD-102X_upgrade2018_realistic_v15

Sample
/DYJetsToLL_M-50_TuneCP5_13TeV-madgraphMLM-pythia8/*-v1/MINIAODSIM
/WJetsToLNu_M-50_TuneCP5_13TeV-madgraphMLM-pythia8/*-v2/MINIAODSIM
/WW_M-50_TuneCP5_13TeV-madgraphMLM-pythia8/*-v2/MINIAODSIM
/WZ_M-50_TuneCP5_13TeV-madgraphMLM-pythia8/*-v3/MINIAODSIM
/ZZ_M-50_TuneCP5_13TeV-madgraphMLM-pythia8/*-v2/MINIAODSIM
/GluGluHToBB_M125_13TeV_amcatnloFXFX-pythia8/*-v1/MINIAODSIM

Table 5: Top background Monte Carlo samples, RunIIAutumn18MiniAOD-102X_upgrade2018_realistic_v15

Sample
/TTJets_TuneCP5_13TeV-madgraphMLM-pythia8/*-v1/MINIAODSIM
/ST_s-channel_4f_hadronicDecays_TuneCP5_13TeV-madgraph-pythia8/*_ext1-v1/MINIAODSIM
/ST_t-channel_top_5f_TuneCP5_13TeV-powheg-pythia8/*-v1/MINIAODSIM
/ST_t-channel_antitop_5f_TuneCP5_13TeV-powheg-pythia8/*-v1/MINIAODSIM
/ST_tW_antitop_5f_inclusiveDecays_TuneCP5_13TeV-powheg-pythia8/*_ext1-v1/MINIAODSIM
/ST_tW_top_5f_inclusiveDecays_TuneCP5_13TeV-powheg-pythia8/*_ext1-v1/MINIAODSIM

Table 6: Monte Carlo sample summary, RunIIAutumn18DRPremix-102X_upgrade2018_realistic_v15

Sample
/QCD_Pt-15to20_MuEnrichedPt5_TuneCP5_13TeV_pythia8/*-v3/MINIAODSIM
/QCD_Pt-20to30_MuEnrichedPt5_TuneCP5_13TeV_pythia8/*-v4/MINIAODSIM
/QCD_Pt-30to50_MuEnrichedPt5_TuneCP5_13TeV_pythia8/*-v3/MINIAODSIM
/QCD_Pt-50to80_MuEnrichedPt5_TuneCP5_13TeV_pythia8/*-v3/MINIAODSIM
/QCD_Pt-80to120_MuEnrichedPt5_TuneCP5_13TeV_pythia8/*_ext1-v2/MINIAODSIM
/QCD_Pt-120to170_MuEnrichedPt5_TuneCP5_13TeV_pythia8/*_ext1-v2/MINIAODSIM
/QCD_Pt-170to300_MuEnrichedPt5_TuneCP5_13TeV_pythia8/*-v3/MINIAODSIM
/QCD_Pt-300to470_MuEnrichedPt5_TuneCP5_13TeV_pythia8/*_ext3-v1/MINIAODSIM
/QCD_Pt-470to600_MuEnrichedPt5_TuneCP5_13TeV_pythia8/*_ext1-v2/MINIAODSIM
/QCD_Pt-600to800_MuEnrichedPt5_TuneCP5_13TeV_pythia8/*-v1/MINIAODSIM
/QCD_Pt-800to1000_MuEnrichedPt5_TuneCP5_13TeV_pythia8/*_ext3-v2/MINIAODSIM
/QCD_Pt-1000toInf_MuEnrichedPt5_TuneCP5_13TeV_pythia8/*-v1/MINIAODSIM
/DYJetsToLL_M-50_TuneCP5_13TeV-madgraphMLM-pythia8/*-v1/MINIAODSIM
/WJetsToLNu_M-50_TuneCP5_13TeV-madgraphMLM-pythia8/*-v2/MINIAODSIM
/WW_M-50_TuneCP5_13TeV-madgraphMLM-pythia8/*-v2/MINIAODSIM
/WZ_M-50_TuneCP5_13TeV-madgraphMLM-pythia8/*-v3/MINIAODSIM
/ZZ_M-50_TuneCP5_13TeV-madgraphMLM-pythia8/*-v2/MINIAODSIM
/GluGluHToBB_M125_13TeV_amcatnloFXFX_pythia8/*-v1/MINIAODSIM
/TTJets_TuneCP5_13TeV-madgraphMLM-pythia8/*-v1/MINIAODSIM
/ST_s-channel_4f_hadronicDecays_TuneCP5_13TeV-madgraph-pythia8/*_ext1-v1/MINIAODSIM
/ST_t-channel_top_5f_TuneCP5_13TeV-powheg-pythia8/*-v1/MINIAODSIM
/ST_t-channel_antitop_5f_TuneCP5_13TeV-powheg-pythia8/*-v1/MINIAODSIM
/ST_tW_antitop_5f_inclusiveDecays_TuneCP5_13TeV-powheg-pythia8/*_ext1-v1/MINIAODSIM
/ST_tW_top_5f_inclusiveDecays_TuneCP5_13TeV-powheg-pythia8/*_ext1-v1/MINIAODSIM
/ggH_HToSSTo4Tau_MH-125_TuneCP5_13TeV-powheg-pythia8/*-v1/MINIAODSIM

3 Physics object definitions

In this section, we provide the definitions of physics objects used in the analysis. We make use of Regions of Interest, muons, taus, and jets.

3.1 Muons

The analysis sources SlimmedMuons from MINIAOD to produce `selectedPatMuons`. Muons require Muon objects require

- $p_T > 12$ GeV to reach BPH trigger plateau
- $|\eta| < 1.5$ due to L1 seed $|\eta|$ cut in BPH HLT path
- Pass the Loose ID criterion (`isLooseMuon`). As described in the Muon POG [52].

The Isolation requirements on muons are discussed in Section 4.

3.2 Jets

The analysis sources SlimmedJets from MINIAOD to produce `selectedJets`. CMS reconstruct jets from calorimeter energy deposits using the anti- k_T clustering algorithm with a distance parameter of $R = 0.4$ [53]. Then, the calojets are inputted into the Particle-Flow (PF) algorithms to produce PFJets. Variables in PFJets class are then slimmed to be saved into MINIAOD files. The analysis uses these SlimmedJets for the jets' b-tagging scores and others. Jet objects require

- $p_T > 20$ GeV
- $|\eta| < 2.4$
- $0 \leq \text{emEnergyFraction} \leq 0.9$
- $0 \leq \text{energyFractionHadronic} \leq 0.9$
- No selected electron or muon within $\Delta R = 0.4$

The energy fraction cuts above are inspired by the recommended Run2 Tight jet-ID cuts for particle flow jets [54–56].

3.3 Taus

The analysis sources `PAT::slimmedTaus` from MINIAOD for MC and `RECO::slimmedTaus` for Data to produce `selectedTaus`. τ objects decay hadronically for 64% of its decay. Hadron-Plus-Strip (HPS) algorithm enables the reconstruction of τ 's hadronic decay. HPS uses PFJets as its starting point. τ 's hadronic decay can be reconstructed with PFJets' charged Hadrons in HCAL and 2 γ s from π^0 in ECAL. Tau objects require

- $p_T > 20$ GeV
- $|\eta| < 2.4$

3.4 Region of Interest

The complete construction procedures of Regions of Interest are detailed in the following subsections.

- Good quality track selection
- Vertex Fitted from pair-wise tracks by V0Fitter in CMSSW
- Cluster the fitted vertices to form a Region of Interest (ROI)

- Look for tracks around $\Delta R = 0.3$ to save ROI isolation information

3.4.1 Tracks

The analysis sources packedPFCandidates and lostTracks from MINIAOD. Track parameters and covariance values will be propagated along the ROI production process and no value should either be infinite or N/A

- `!isinf(tracks.parameter) !isnan(tracks.parameter)`
- `!isinf(tracks.covariance) !isnan(tracks.covariance)`
- Number of valid hits > 3
- $p_T > 0.35$
- Track $IPSig_{XY} > 2$.
- Track $IPSig_Z > -1$.
- Track normalized $\chi^2 < 10$.

3.4.2 Vertex Fitter

The analysis sources offlineBeamspot from MINIAOD for beamspot reference. Vertex fitter is KalmanVertexFitter with cuts on the vertex

- Vertex $\chi^2 < 6.63$
- Transverse Decay distance significance > 15 .
- $V0_{mass} < 13000 \text{ GeV}$
- $\cos(\theta_{XY})$ between x and p of V0 candidate > 0
- $\cos(\theta_{XZ})$ between x and p of V0 candidate > -2

3.4.3 ROI formation

Fitted V0s are clustered to form a Region of Interest (ROI). These ROIs have cuts on their parameters as below.

- Radius of ROI $< 1 \text{ cm}$
- Annulus $\Delta R < 0.3$

4 Event Selection, Signal and Control Regions

The signal process of the analysis contains SM τ fermions for its final state. In order to exploit the leptonic decay of τ lepton, specifically with muon final state for clean signal, the B-Parking triggers are used. CMS implemented the B-Parking trigger starting in 2018 of Run 2 for research of lepton universalities. For research of $R(K^*, D^*)$, muonic final state of B mesons are desired. B trigger requires a soft muon with modest displacement (impact parameter) from primary vertex due to b-quark's long lifetime. B Parking HLT requires a muon with 7-12 GeV with IP 3-6. pp collisions in LHC produce extremely enormous amount of data, which could be triggered by paths above. Current CPU capacity of CMS is limited and not capable of reconstructing the entire event at such high rate at HLT level. CMS scouts events, which passed L1 trigger, and writes them to a temporary dataset. Later, full HLT and RECO schemes are implemented and served as a B-Parking dataset. The prescale factor for HLT is 5-6.

4.1 Global Tags

Table 7: Data and MC Global tags used 2018

Data 2018	106X.dataRun2_v29
MC 2018	106X_upgrade2018_realistic_v11_L1v1

4.2 Trigger Strategy

We utilize the B-Parking triggers collecting data at L1 and HLT for 2018. The HLT paths of these triggers are listed in Tables 8. We observe that the triggers become efficient around the nominal trigger thresholds.

Table 8: HLT trigger paths used in the analysis 2018.

Data sample	Trigger
ParkingBPH*-Run2018A	HLT_Mu9_IP6_part*
ParkingBPH*-Run2018B	HLT_Mu12_IP6_part*
ParkingBPH*-Run2018C	HLT_Mu12_IP6_part*
ParkingBPH*-Run2018D	HLT_Mu12_IP6_part*

References

- [1] D0 Collaboration, “Search for High Mass Top Quark Production in pp Collisions at $s = 1.8$ TeV”, *Phys. Lett.* **74** (1995) 12, doi:10.1103/PhysRevLett.74.2422, arXiv:9411001.
- [2] CDF Collaboration, “Observation of Top Quark Production in pp Collisions with the Collider Detector at Fermilab”, *Phys. Lett.* **74** (1995) 21, doi:10.1103/PhysRevLett.74.2626, arXiv:9503002.
- [3] CMS Collaboration, “Observation of a New Boson at a Mass of 125 GeV with the CMS Experiment at the LHC”, *Phys. Lett.* **B716** (2012) 30–61, doi:10.1016/j.physletb.2012.08.021, arXiv:1207.7235.
- [4] ATLAS Collaboration, “Observation of a new particle in the search for the Standard Model Higgs boson with the ATLAS detector at the LHC”, *Phys. Lett.* **B716** (2012) 1–29, doi:10.1016/j.physletb.2012.08.020, arXiv:1207.7214.
- [5] Super-Kamiokande Collaboration, “Evidence for Oscillation of Atmospheric Neutrinos”, *Phys. Lett.* **81** (1998) 9, doi:10.1103/PhysRevLett.81.1562, arXiv:9807003.
- [6] M. Baumgart et al., “Non-Abelian Dark Sectors and Their Collider Signatures”, *JHEP* **04** (2009) 014, doi:10.1088/1126-6708/2009/04/014, arXiv:0901.0283.
- [7] D. E. Kaplan, M. A. Luty, and K. M. Zurek, “Asymmetric Dark Matter”, *Phys. Rev.* **D79** (2009) 115016, doi:10.1103/PhysRevD.79.115016, arXiv:0901.4117.
- [8] Y. F. Chan, M. Low, D. E. Morrissey, and A. P. Spray, “LHC Signatures of a Minimal Supersymmetric Hidden Valley”, *JHEP* **05** (2012) 155, doi:10.1007/JHEP05(2012)155, arXiv:1112.2705.
- [9] K. R. Dienes and B. Thomas, “Dynamical Dark Matter: I. Theoretical Overview”, *Phys. Rev.* **D85** (2012) 083523, doi:10.1103/PhysRevD.85.083523, arXiv:1106.4546.
- [10] K. R. Dienes, S. Su, and B. Thomas, “Distinguishing Dynamical Dark Matter at the LHC”, *Phys. Rev.* **D86** (2012) 054008, doi:10.1103/PhysRevD.86.054008, arXiv:1204.4183.
- [11] Y. Cui and B. Shuve, “Probing Baryogenesis with Displaced Vertices at the LHC”, *JHEP* **02** (2015) 049, doi:10.1007/JHEP02(2015)049, arXiv:1409.6729.
- [12] Z. Chacko, H.-S. Goh, and R. Harnik, “The Twin Higgs: Natural electroweak breaking from mirror symmetry”, *Phys. Rev. Lett.* **96** (2006) 231802, doi:10.1103/PhysRevLett.96.231802, arXiv:hep-ph/0506256.
- [13] G. Burdman, Z. Chacko, H.-S. Goh, and R. Harnik, “Folded supersymmetry and the LEP paradox”, *JHEP* **02** (2007) 009, doi:10.1088/1126-6708/2007/02/009, arXiv:hep-ph/0609152.
- [14] H. Cai, H.-C. Cheng, and J. Terning, “A Quirky Little Higgs Model”, *JHEP* **05** (2009) 045, doi:10.1088/1126-6708/2009/05/045, arXiv:0812.0843.
- [15] N. Craig, A. Katz, M. Strassler, and R. Sundrum, “Naturalness in the Dark at the LHC”, *JHEP* **07** (2015) 105, doi:10.1007/JHEP07(2015)105, arXiv:1501.05310.

- [16] D. Curtin and C. B. Verhaaren, “Discovering Uncolored Naturalness in Exotic Higgs Decays”, *JHEP* **12** (2015) 072, doi:10.1007/JHEP12(2015)072, arXiv:1506.06141.
- [17] C. Csaki, E. Kuflik, S. Lombardo, and O. Slone, “Searching for displaced Higgs boson decays”, *Phys. Rev.* **D92** (2015), no. 7, 073008, doi:10.1103/PhysRevD.92.073008, arXiv:1508.01522.
- [18] CDF Collaboration, “Search for heavy metastable particles decaying to jet pairs in $p\bar{p}$ collisions at $\sqrt{s} = 1.96$ TeV”, *Phys. Rev.* **D85** (2012) 012007, doi:10.1103/PhysRevD.85.012007, arXiv:1109.3136.
- [19] D0 Collaboration, “Search for Resonant Pair Production of long-lived particles decaying to b anti- b in p anti- p collisions at $s^{1/2} = 1.96$ -TeV”, *Phys. Rev. Lett.* **103** (2009) 071801, doi:10.1103/PhysRevLett.103.071801, arXiv:0906.1787.
- [20] ATLAS Collaboration, “Search for a light Higgs boson decaying to long-lived weakly-interacting particles in proton-proton collisions at $\sqrt{s} = 7$ TeV with the ATLAS detector”, *Phys. Rev. Lett.* **108** (2012) 251801, doi:10.1103/PhysRevLett.108.251801, arXiv:1203.1303.
- [21] LHCb Collaboration, “Search for long-lived particles decaying to jet pairs”, *Eur. Phys. J.* **C75** (2015), no. 4, 152, doi:10.1140/epjc/s10052-015-3344-6, arXiv:1412.3021.
- [22] ATLAS Collaboration, “Search for long-lived, weakly interacting particles that decay to displaced hadronic jets in proton-proton collisions at $\sqrt{s} = 8$ TeV with the ATLAS detector”, *Phys. Rev.* **D92** (2015), no. 1, 012010, doi:10.1103/PhysRevD.92.012010, arXiv:1504.03634.
- [23] ATLAS Collaboration, “Search for massive, long-lived particles using multitrack displaced vertices or displaced lepton pairs in pp collisions at $\sqrt{s} = 8$ TeV with the ATLAS detector”, *Phys. Rev.* **D92** (2015), no. 7, 072004, doi:10.1103/PhysRevD.92.072004, arXiv:1504.05162.
- [24] CMS Collaboration, “Search for long-lived neutral particles decaying to quark-antiquark pairs in proton-proton collisions at $\sqrt{s} = 8$ TeV”, *Phys. Rev. D* **91** (Jan, 2015) 012007, doi:10.1103/PhysRevD.91.012007.
- [25] ATLAS Collaboration, “Search for pair-produced long-lived neutral particles decaying in the ATLAS hadronic calorimeter in pp collisions at $\sqrt{s} = 8$ TeV”, *Phys. Lett.* **B743** (2015) 15–34, doi:10.1016/j.physletb.2015.02.015, arXiv:1501.04020.
- [26] LHCb Collaboration, “Updated search for long-lived particles decaying to jet pairs”, *Eur. Phys. J. C* **77** (2017), no. 12, 812, doi:10.1140/epjc/s10052-017-5178-x, arXiv:1705.07332.
- [27] LHCb Collaboration, “Search for massive long-lived particles decaying semileptonically in the LHCb detector”, *Eur. Phys. J. C* **77** (2017), no. 4, 224, doi:10.1140/epjc/s10052-017-4744-6, arXiv:1612.00945.
- [28] LHCb Collaboration, “Search for long-lived heavy charged particles using a ring imaging Cherenkov technique at LHCb”, *Eur. Phys. J. C* **75** (2015), no. 12, 595, doi:10.1140/epjc/s10052-015-3809-7, arXiv:1506.09173.

- [29] CMS Collaboration, “Search for new long-lived particles at $\sqrt{s} = 13$ TeV”, *Phys. Lett. B* **780** (2018) 432–454, doi:10.1016/j.physletb.2018.03.019, arXiv:1711.09120.
- [30] CMS Collaboration, “Search for long-lived particles with displaced vertices in multijet events in proton-proton collisions at $\sqrt{s} = 13$ TeV”, *Phys. Rev. D* **98** (2018), no. 9, 092011, doi:10.1103/PhysRevD.98.092011, arXiv:1808.03078.
- [31] CMS Collaboration, “Search for long-lived particles decaying into displaced jets in proton-proton collisions at $\sqrt{s} = 13$ TeV”, *Phys. Rev. D* **99** (2019), no. 3, 032011, doi:10.1103/PhysRevD.99.032011, arXiv:1811.07991.
- [32] CMS Collaboration, “Search for long-lived particles using nonprompt jets and missing transverse momentum with proton-proton collisions at $\sqrt{s} = 13$ TeV”, *Phys. Lett. B* **797** (2019) 134876, doi:10.1016/j.physletb.2019.134876, arXiv:1906.06441.
- [33] CMS Collaboration, “Search for new particles decaying to a jet and an emerging jet”, *JHEP* **02** (2019) 179, doi:10.1007/JHEP02(2019)179, arXiv:1810.10069.
- [34] CMS Collaboration Collaboration, “Search for long-lived particles decaying into displaced jets”, Technical Report CMS-PAS-EXO-19-021, CERN, Geneva, 2020.
- [35] ATLAS Collaboration, “Search for the Higgs boson produced in association with a vector boson and decaying into two spin-zero particles in the $H \rightarrow aa \rightarrow 4b$ channel in pp collisions at $\sqrt{s} = 13$ TeV with the ATLAS detector”, *JHEP* **10** (2018) 031, doi:10.1007/JHEP10(2018)031, arXiv:1806.07355.
- [36] ATLAS Collaboration, “Search for long-lived particles in final states with displaced dimuon vertices in pp collisions at $\sqrt{s} = 13$ TeV with the ATLAS detector”, *Phys. Rev. D* **99** (2019), no. 1, 012001, doi:10.1103/PhysRevD.99.012001, arXiv:1808.03057.
- [37] ATLAS Collaboration, “Search for the Production of a Long-Lived Neutral Particle Decaying within the ATLAS Hadronic Calorimeter in Association with a Z Boson from pp Collisions at $\sqrt{s} = 13$ TeV”, *Phys. Rev. Lett.* **122** (2019), no. 15, 151801, doi:10.1103/PhysRevLett.122.151801, arXiv:1811.02542.
- [38] ATLAS Collaboration, “Search for long-lived particles produced in pp collisions at $\sqrt{s} = 13$ TeV that decay into displaced hadronic jets in the ATLAS muon spectrometer”, *Phys. Rev. D* **99** (2019), no. 5, 052005, doi:10.1103/PhysRevD.99.052005, arXiv:1811.07370.
- [39] ATLAS Collaboration, “Search for heavy long-lived multicharged particles in proton-proton collisions at $\sqrt{s} = 13$ TeV using the ATLAS detector”, *Phys. Rev. D* **99** (2019), no. 5, 052003, doi:10.1103/PhysRevD.99.052003, arXiv:1812.03673.
- [40] ATLAS Collaboration, “Search for heavy charged long-lived particles in the ATLAS detector in 36.1 fb^{-1} of proton-proton collision data at $\sqrt{s} = 13$ TeV”, *Phys. Rev. D* **99** (2019), no. 9, 092007, doi:10.1103/PhysRevD.99.092007, arXiv:1902.01636.
- [41] ATLAS Collaboration, “Search for long-lived neutral particles in pp collisions at $\sqrt{s} = 13$ TeV that decay into displaced hadronic jets in the ATLAS calorimeter”, *Eur. Phys. J. C* **79** (2019), no. 6, 481, doi:10.1140/epjc/s10052-019-6962-6, arXiv:1902.03094.

- [42] ATLAS Collaboration, “Search for heavy neutral leptons in decays of W bosons produced in 13 TeV pp collisions using prompt and displaced signatures with the ATLAS detector”, *JHEP* **10** (2019) 265, doi:10.1007/JHEP10(2019)265, arXiv:1905.09787.
- [43] ATLAS Collaboration, “Search for Magnetic Monopoles and Stable High-Electric-Charge Objects in 13 TeV Proton-Proton Collisions with the ATLAS Detector”, *Phys. Rev. Lett.* **124** (2020), no. 3, 031802, doi:10.1103/PhysRevLett.124.031802, arXiv:1905.10130.
- [44] ATLAS Collaboration, “Search for displaced vertices of oppositely charged leptons from decays of long-lived particles in pp collisions at $\sqrt{s}=13$ TeV with the ATLAS detector”, *Phys. Lett. B* **801** (2020) 135114, doi:10.1016/j.physletb.2019.135114, arXiv:1907.10037.
- [45] ATLAS Collaboration, “Search for long-lived neutral particles produced in pp collisions at $\sqrt{s}=13$ TeV decaying into displaced hadronic jets in the ATLAS inner detector and muon spectrometer”, *Phys. Rev. D* **101** (2020), no. 5, 052013, doi:10.1103/PhysRevD.101.052013, arXiv:1911.12575.
- [46] ATLAS Collaboration, “Search for light long-lived neutral particles produced in pp collisions at $\sqrt{s}=13$ TeV and decaying into collimated leptons or light hadrons with the ATLAS detector”, *Eur. Phys. J. C* **80** (2020), no. 5, 450, doi:10.1140/epjc/s10052-020-7997-4, arXiv:1909.01246.
- [47] CMS Collaboration, “Search for long-lived particles produced in association with a Z boson in proton-proton collisions at $s=13$ TeV”, *JHEP* (2021) 36, doi:10.1103/PhysRevLett.74.2422, arXiv:2110.13218.
- [48] B. T. Shufang Su, “The LHC Discovery Potential of a Leptophilic Higgs”, *Phys.Rev.D79:095014,2009* (2009) 25, doi:10.1103/PhysRevD.79.095014, arXiv:0903.0667.
- [49] G. P. R. T. S. Heinemeyer, C. Mariotti et al., “Handbook of LHC Higgs Cross Sections: 3. Higgs Properties”, doi:10.5170/CERN-2013-004, arXiv:1307.1347.
- [50] GEANT4 Collaboration, “GEANT4: A Simulation toolkit”, *Nucl. Instrum. Meth. A* **506** (2003) 250–303, doi:10.1016/S0168-9002(03)01368-8.
- [51] CMS Collaboration, Khachatryan et al., “Physics Performance Datasets – PPD Run2 Analysis Recipe Summary”, 2020, <https://twiki.cern.ch/twiki/bin/viewauth/CMS/PdmVAnalysisSummaryTable>.
- [52] CMS Collaboration, Khachatryan et al., “Muon POG – Muon Identification Run2”, 2020, <https://twiki.cern.ch/twiki/bin/viewauth/CMS/SWGuideMuonIdRun2>.
- [53] M. Cacciari, G. P. Salam, and G. Soyez, “The anti- k_t jet clustering algorithm”, *JHEP* **04** (2008) 063, doi:10.1088/1126-6708/2008/04/063, arXiv:0802.1189.
- [54] CMS Collaboration, Khachatryan et al., “Jet Identification Run2 – 2016”, 2020, <https://twiki.cern.ch/twiki/bin/view/CMS/JetID13TeVRun2016>.
- [55] CMS Collaboration, Khachatryan et al., “Jet Identification Run2 – 2017”, 2020, <https://twiki.cern.ch/twiki/bin/view/CMS/JetID13TeVRun2017>.
- [56] CMS Collaboration, Khachatryan et al., “Jet Identification Run2 – 2018”, 2020, <https://twiki.cern.ch/twiki/bin/view/CMS/JetID13TeVRun2018>.